JAMA Ophthalmology | Original Investigation

Founder Homozygous Nonsense *CREB3* Variant and Variable-Onset Retinal Degeneration

Manar Salameh, MSc; Ghadeer Abu Tair, MSc; Samira Mousa, BSc; Alexey Obolensky, PhD; Anand Swaroop, PhD; Susanne Roosing, PhD; Eedy Mezer, MD; Shiri Soudry, MD; Marianthi Karali, PhD; Francesca Simonelli, MD; Sandro Banfi, MD; Eyal Banin, MD, PhD; Tamar Ben-Yosef, PhD; Dror Sharon, PhD; Samer Khateb, MD, PhD

IMPORTANCE Uncovering the genetic basis of inherited retinal diseases (IRDs) can enhance both diagnostic accuracy and the development of targeted treatment strategies.

OBJECTIVE To evaluate the association between a homozygous nonsense variant in *CREB3* with IRDs.

DESIGN, SETTING, AND PARTICIPANTS Thirteen patients with a clinical diagnosis of retinitis pigmentosa or cone-rod degeneration were analyzed by whole-genome sequencing (WGS) and whole-exome sequencing (WES). Clinically, patients presented with 2 main phenotypes, rod-cone and cone-rod dystrophies, demonstrating variable electrophysiological and fundoscopic findings. Expression analysis was performed on patient-derived skin fibroblasts using the reverse transcription–polymerase chain reaction and Western blot analysis, and by interrogating previously published retinal single-cell RNA sequence data. Immunohistochemistry staining was performed on wild-type mouse retinal sections using an anti-CREB3 antibody. Patients with variable phenotypes of IRDs were recruited from 3 medical centers in Israel and Italy. Ophthalmologists clinically diagnosed patients at the relevant medical centers and referred them for genetic screening. WES and WGS were performed at different national and international centers, and the findings of the previously unreported gene were shared between investigators.

EXPOSURES *CREB3* and IRDs.

MAIN OUTCOMES AND MEASURES The main outcome was evidence supporting an association between *CREB3* and IRD. Measures included WES, WGS, and immunohistochemistry staining.

RESULTS A founder homozygous nonsense variant in *CREB3* (c.881G>A, p.Trp294*) was identified in 13 patients from 4 unrelated families; 12 descendent from North-African Jewish origins and 1 from Italian origins. All patients manifested retinal degeneration with varying ages at onset. In patient-derived fibroblasts, the variant mRNA transcript generated a truncated CREB3 protein. Expression analysis and immunohistochemistry staining revealed CREB3 RNA and protein expression in various retinal cell types, indicating its vital role in photoreceptor function.

CONCLUSIONS AND RELEVANCE This study found an association between *CREB3* and IRDs. *CREB3* was previously shown to be upregulated following ultraviolet radiation. This might contribute to the extensive clinical variability observed in this relatively large cohort of homozygous patients with the same truncated variant.

Invited Commentary

Supplemental content

Author Affiliations: Author affiliations are listed at the end of this article.

Corresponding Author: Samer Khateb; MD, PhD, Department of Ophthalmology, Hadassah University Medical Center, Faculty of Medicine, the Hebrew University of Jerusalem, Jerusalem, Israel, 91120 (samer.khateb@mail.huji.ac.il).

JAMA Ophthalmol. doi:10.1001/jamaophthalmol.2025.2187
Published online July 17, 2025.

Inherited retinal diseases (IRDs) constitute a large group of rare diseases characterized by degeneration of photoreceptors and/or the retinal pigment epithelium, resulting in vision impairment and, often, blindness. IRDs are clinically and genetically heterogeneous, with disease-associated variants found in more than 300 genes, with various inheritance patterns (autosomal dominant, autosomal recessive, X-linked, or mitochondrial, in most cases).[1]

In terms of clinical presentation, there are more than 50 distinct IRD phenotypes, including rod-dominated diseases, cone-dominated diseases, generalized retinal degenerations, and vitreoretinopathies.[1] Based on an analysis of genomic data of unaffected individuals, we previously reported that approximately 5.5 million people are expected to be affected by autosomal recessive IRDs worldwide.[2] In addition, we reported carrier frequency of all autosomal recessive IRD-related variants combined reaches extremely high levels of approximately 1 in 3 individuals worldwide. The most common IRD subtype is retinitis pigmentosa (OMIM 268000), with an average disease prevalence of approximately 1 in 4500 individuals and even higher in regions with a high consanguinity.[3]

Although a large number of IRD-associated genes have been reported thus far, additional previously unreported genes are being identified mainly due to the development of next-generation sequencing-based techniques, such as whole-exome and -genome sequencing (WES and WGS, respectively).[4-8] Nonetheless, the diagnostic genetic yield of IRDs following WES and WGS analyses is still limited, with the genetic etiology being identified in 50% to 70% of studied cases.[9-12] The missing heritability of the unsolved proportion can be identified within less explored regions of known IRD genes (eg, promoters, enhancers, untranslated region, and introns), as reported for many IRD genes, including *CNGB3*[13] and *ELOVL4*,[14] or in genes that were not reported previously to be associated with IRD.

Homozygosity mapping was first introduced in 1987 by Lander and Botstein[15] as a tool that can be used to trace the inheritance of a chromosomal region from an ancestor through consanguineous heterozygous parents to a homozygous patient. Genomic homozygous regions can be either homozygous by state (ie, the same disease-causing variant was inherited from unrelated parents) or autozygous identical by descent due to consanguinity or intracommunity marriages. Such nonrandom matings lead to higher levels of homozygosity, increasing the prevalence of autosomal recessive diseases. The combination of homozygosity mapping and next-generation sequencing enhances the identification of the disease underlying variation in consanguineous families,[16,17] as well as in families where no consanguinity was reported but the parents share a common distantly related ancestor.[18]

Here we report the identification of a homozygous nonsense variant (c.881G>A) in *CREB3* (cyclic AMP response element binding protein-3; OMIM *606443) in 13 affected individuals from 4 unrelated families with IRD, 3 of which were of North-African Jewish ancestry and 1 Italian, that led to retinal degeneration. The variant introduces a premature stop codon (p.Trp294*), leading to a truncated CREB3 protein, affecting its cellular localization. Taken together, our data suggest that *CREB3*, which has not been previously found to be associated with retinal disease, is an IRD-associated gene.

Key Points

Question Is *CREB3* involved in inherited retinal diseases (IRDs)?

Findings In this cohort study including 13 patients, a homozygous nonsense variant in *CREB3* was associated with variable IRD phenotypes in 3 families of North-African Jewish descent and 1 Italian family.

Meaning Whole-genome and whole-exome sequencing enabled the identification and verification of an association between *CREB3* and IRDs; *CREB3* should be included in the genetic analysis of IRD cases with retinitis pigmentosa with or without macular involvement.

Methods

Patient Recruitment

Patients with IRD and their healthy family members were recruited from the Department of Ophthalmology at Hadassah Medical Center in Jerusalem, Israel, and the Eye Clinic of the Multidisciplinary Department of Medical, Surgical and Dental Sciences at the University of Campania Luigi Vanvitelli, Naples, Italy. The tenets of the Declaration of Helsinki were followed; the study was approved by the institutional review board of the respective institutions, including the Hadassah University Medical Center, and before the donation of a blood sample, written informed consent was obtained from all participants. Participants did not receive any compensation or incentives for their participation. This study was reported according to the Strengthening the Reporting of Observational Studies in Epidemiology (STROBE) reporting guideline.

Statistical Analysis

Materials and methods are detailed in the eMethods in Supplement 1. Briefly, patient recruitment was conducted per the tenets of the Declaration of Helsinki. All clinical examinations, including ocular examination and electrophysiological testing, were performed by ophthalmologists from the collaborators' centers. Genetic analyses were performed on blood samples extracted from patients to perform WES or WGS. Homozygosity mapping was performed using Automap and Franklin platforms. For patient-derived skin fibroblasts, skin biopsies were collected from patients or control individuals under sterile and suitable conditions, and when fibroblast growth was noticed to reach 100% confluency, RNA and proteins were extracted. For expression analysis, Western blot analysis on protein extracted from fibroblasts, 30 µg of protein lysate of wild-type and variant samples were run on a 10% acrylamide gel. Nonsense-mediated mRNA decay for the mutated or wild-type transcript was performed using reverse transcription–polymerase chain reaction RT-PCR using suitable primers as detailed in eTable 1 in Supplement 1. Immunohistochemical staining was performed using CREB3 antibody (MBS9133614) on wild-type mouse retina FFPE tissue.

Figure 1. Pedigrees of 4 Families Harboring the *CREB3* c.881G>A Homozygous Pathogenic Variant

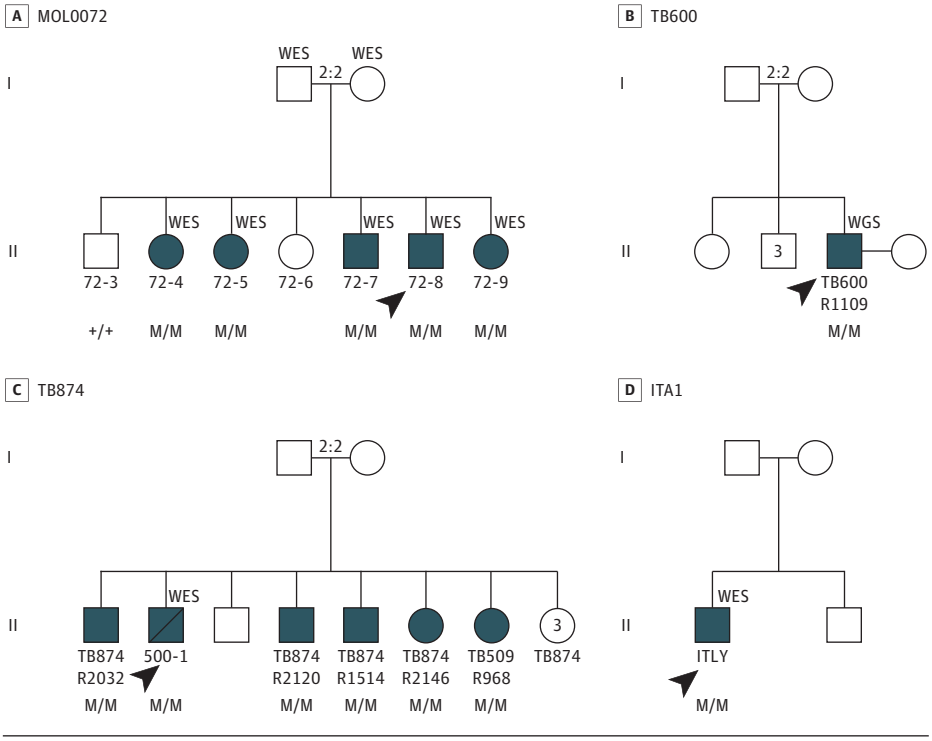

Solid squares denote affected individuals, and arrows indicate index cases. A double line indicates consanguinity, and numbers refer to its level (eg, 2:2 represents first-cousin marriage). WES indicates whole-exome sequencing; WGS, whole-genome sequencing.

Results

Clinical Description of Recruited Patients

Four families with IRDs, including 3 consanguineous North-African Jewish families (MOL0072, TB874, and TB600) and a nonconsanguineous Italian family (ITA1), were recruited for this study. This cohort consists of a total of 13 affected individuals (MOL0072 with 5 patients, TB874 with 6 patients, TB600 and ITA1 with 1 patient each) (**Figure 1**). As detailed below, all patients were found to be homozygous for the same nonsense variant, c.881G>A, p.Trp294* in *CREB3* (eFigure 1A in Supplement 1). Detailed case reports are provided in the eAppendix in Supplement 1. Family MOL0072 comprised 5 affected individuals with rod-cone dystrophy with extremely variable age at onset and disease severity. Individuals MOL0072-5, 7, 8, and 9 developed visual disturbances around their 30s. Clinically, patients presented reduced visual acuity (mean [SD] best-corrected visual acuity [BCVA], 0.37 [0.37] at a mean [SD] age of 44 [3.53] years) (**Table**) along with diffuse peripheral retinal atrophy combined with bone spicule–like pigmentations surrounding the fovea (**Figure 2**A-D; eFigure 3A-D, G-H in Supplement 1). Optical coherence tomography showed diffuse retinal atrophy with a small preserved foveal island of the ellipsoid zone (Figure 2E and F; eFigure 3E and F in Supplement 1). Full-field electroretinography (ffERG) responses were severely reduced and compatible with rod-cone dystrophy (Table). Visual fields for patients MOL0072-7, 8, and 9 were extremely constricted, with a mean of 20 central degrees at age 36 years. Patient MOL0072-4 was asymptomatic when examined initially at age 35 years, with a BCVA of 0.90 in both eyes and completely normal retinal examination and electrophysiological tests (Table). A clinical reexamination 11 years later showed slight visual disturbances, subtle peripheral retinal atrophic changes, seen as heterogenic fundus autofluorescence appearance, and completely normal retinal layering of the macula as seen on optical coherence tomography. Of note, repeated ffERG demonstrated slightly reduced mixed rod-cone responses, indicating the appearance of rod-cone dystrophy at age 46 years.

Family TB874 consisted of 6 affected individuals (Figure 1) with variable age at onset, ranging from 21 to 60 years, and 1 of whom was initially diagnosed with pigmented paravenous retinochoroidal atrophy. The mean (range) BCVA was 0.28 (0.2-0.40) at a mean (range) age of 51 (30-65) years with atrophy and peripapillary pigmentary changes, surrounding also the arcades, as seen in color and fundus autofluorescence images (eFigure 3I-L in Supplement 1). ffERG showed overall diminished rod and cone responses compatible with cone-rod dystrophy.

Family TB600 had a single affected individual (R1109) who had visual impairment since age 15 years, with slow deterioration over the years. He was initially examined at age 50 years with a BCVA of 0.25 in both eyes and a fundus appearance of maculopathy; however, ffERG testing at age 61 years showed no photopic and scotopic responses. His BCVA deteriorated to 1/60 by age 67 years.

Family ITA1 was nonconsanguineous, descending from Italian origins, with a sporadic affected 36-year-old male individual (ITA1:II 1) (Figure 1). He was complaining of nyctalopia starting at age 27 years and was diagnosed with nonsyndromic retinitis pigmentosa. The mean (SD) BCVA was

Table. Clinical Features of Patients Who Are Homozygous for *CREB3* c.881G>A

Patient No.	Phenotype	Age at onset, y	Age at test, y	Mean Snellen BCVA	Cone flicker, μV; msec	Mixed cone-rod response, a-wave/ b-wave, μV	Rod response, μV	Color vision	VF of both eyes[a]
MOL0072-4[b]	RCD	46	35	0.9	76; 31	131; 347	295	Normal	Goldmann 130° at age 36 y; target 4I
			46	1.0	48; 30	92; 217	134	Normal	
MOL0072-5[b]	RCD	12	12	0.50	Normal	Moderate-severe	NA	NA	SITA-Fast 30-2 at age 34 y; diffuse suppression with C-shape scotoma in the temporal hemifield, both eyes
			34	0.65	84; 36	121; 130	Extinct	Normal	
			48	0.40	NA	NA	NA	NA	
MOL0072-7[b]	RCD	10	30	0.11	5; 43	24; 69	Extinct	Tritanopia	Goldmann 10° at age 30 y; target 4V
			39	0.08	NA	NA	NA	NA	
MOL0072-8[b]	RCD	8	8	0.21	NA	NA	NA	NA	Goldmann 10° at age 36 y; target 4V
			36	0.18	Extinct	Extinct	Extinct	Tritanopia	
			45	0.25	NA	NA	NA	NA	
MOL0072-9[b]	RCD	15	16	NA	NA	NA	NA	NA	Goldmann 30°-40° at age 42 y; target 4V
			34	0.12	37; 38	43; 79	Extinct	Tritanopia	
			42	0.14	NA	NA	NA	NA	
TB874 II:2 (MOL0500-1)[c]	CRD	55	58	0.40	38/40	130/78	Extinct	Tritanopia	Goldmann 100° at age 58 y; target 4V
TB874 II:1 (R2032)[c]	CRD	60	65	0.21	15; 39	30; 17	Extinct	NA	NA
			66	0.10	NA	NA	NA	NA	
TB874 II:5 (R1514)[c]	CRD	21	30	0.20	NA	NA	NA	NA	NA
			31	0.30	NA	NA	NA	NA	
			61	0.05	47; 32	246; 384	204	NA	
*TB874 II:6 (R2146)[c]	CRD		50	0.55	Extinct	Extinct	Extinct	NA	NA
*TB874 II:4 (R2120)[c]	RCD		57	0.50	29/40	32/47	Extinct	NA	SITA-Standard 24-2: 15 central degrees at age 57 y
TB600 (R1109)[c]	CRD with early macular involvement	15	50	0.25	NA	NA	NA	NA	NA
			61	NA	Extinct	Extinct	Extinct	NA	
			67	0.02	NA	NA	NA	NA	
ITA-1	RP	27	28	0.7	69; 30	46; 56	Extinct	Normal	Goldmann 110°; (target V); 110° (target V)
			36	0.6	70; 35	27; 54	Extinct	Normal	

Abbreviations: BCVA, best-corrected visual acuity; CRD, cone-rod dystrophy; NA, not available; RCD, rod-cone dystrophy; RP, retinitis pigmentosa; VF, visual field.

[a] Stimulus size is presented on a scale from 0 to 5, with 5 being the largest; luminance on a scale from I (dim) to V (bright).

[a] Normal ranges: cone flicker 30 Hz (60 μV, 33 msec), mixed cone-rod response (b-wave: 400 μV).

[b] Normal ranges: light-adapted single electroretinography (ERG) (minimum, 70; maximum, 32), light-adapted flicker ERG (minimum, 60; maximum, 31), dark-adapted blue light ERG (minimum, 55), dark-adapted red light ERG (minimum, 60), dark-adapted bright flash ERG (a-wave minimum, 190; b-wave minimum, 250); sum oscillatory (minimum, 90).

0.80 (0.14), and fundus examination revealed diffuse retinal pigment epithelium atrophy, bone spicule-like pigmentations in the midperiphery, and cystoid macular edema. Fundus autofluorescence demonstrates a hyperautofluorescent ring encircling the macular region (eFigure 3M-P in Supplement 1). Horizontal optical coherence tomography sections revealed diffuse retinal atrophy with a relatively preserved foveal island of ellipsoid zone, along with mild cystoid macular edema (eFigure 3Q-R in Supplement 1). ffERG responses were compatible with rod-cone dystrophy.

WES and WGS Genetic Analyses

Seven affected members belonging to the 4 unrelated families were analyzed by WES (6 individuals) or WGS (1 individual) (Figure 1). No disease-causing variants were identified in known IRD genes in this analysis. We identified a single suspected homozygous pathogenic variant (c.881G>A, p.Trp294*) in exon 9 of *CREB3* (NM_006368.5) encoding the cyclic AMP–responsive element binding protein 3 (eFigure 1A in Supplement 1). Segregation analysis revealed a total of 13 affected individuals across these 4 families who were homozygous for this variant (Figure 1). Since 12 of the 13 individuals were of North African Jewish descent, we suspected that this variant is a founder variant. The *CREB3* gene is located on the short arm of chromosome 9, where it spans a region of 4.5 Kb (chr9:35,732,317 - 35,737,005; hg19). Homozygosity mapping on WES data of 7 individuals who were homozygous for c.881G>A revealed that the 6 individuals of North African Jewish descent shared an identical haplotype of approximately 4.6 Mb (chr9:35,107,857 to chr9:39,796,277; hg19) encompassing *CREB3* (eFigure 1B in Supplement 1), while no other shared haplotypes of more than 0.1 Mb were identified. On the other

Figure 2. Multimodal Retinal Imaging of Patient MOL0072-5 (Aged 34 Years), Homozygous for the Disease-Causing Variant c.881G>A in *CREB3*

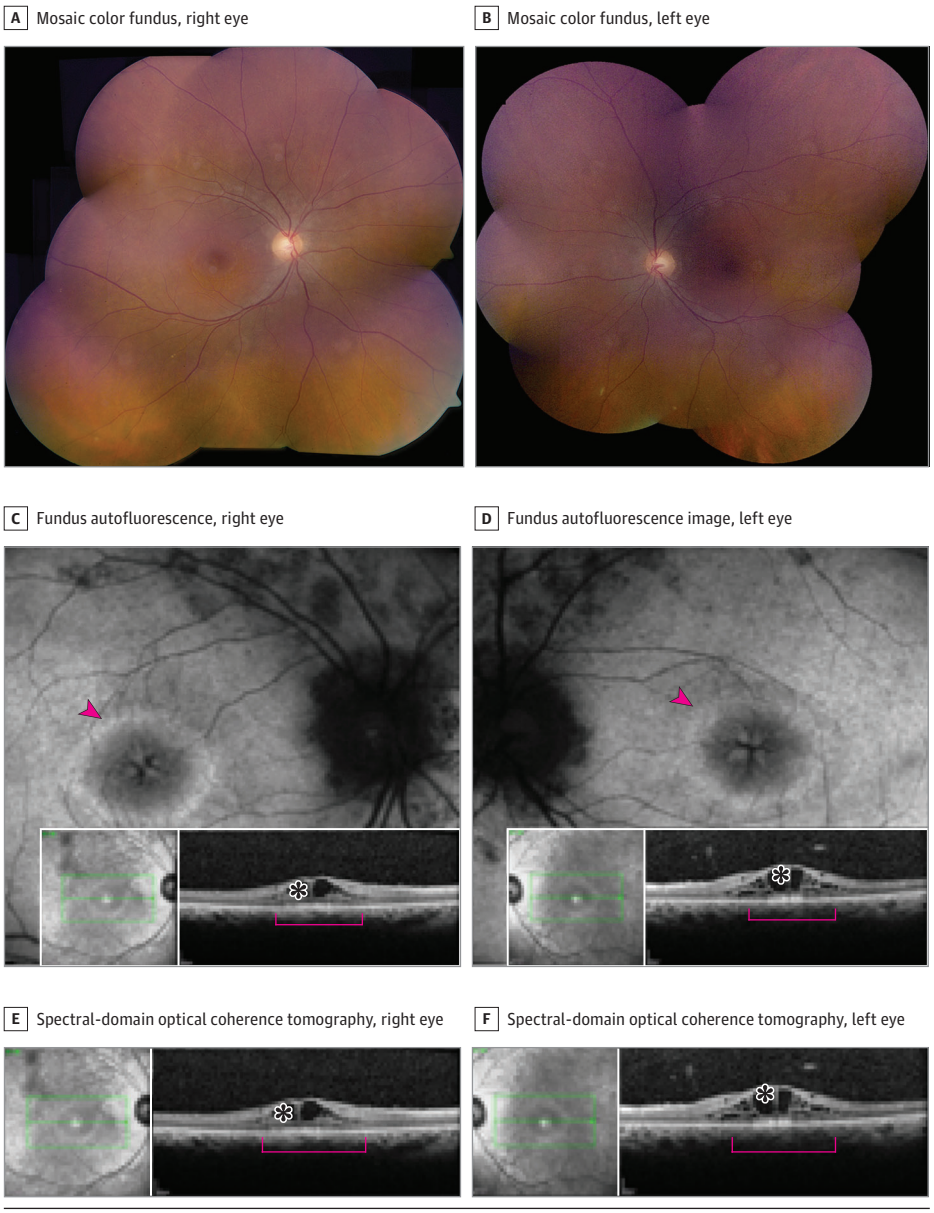

A and B, Mosaic color fundus images show retinal degeneration in the midperiphery combined with vascular attenuation. C and D, Corresponding fundus autofluorescence images reveal a central area of petaloid-shaped heterogenous autofluorescence, compatible with cystoid macular edema, surrounded by a parafoveal ring of hyperautofluorescence (arrowheads), indicating the margins of the encroaching retinal atrophy. The hypoautofluorescent patches over the vascular arcades demonstrate the midperipheral retinal atrophy. E and F, Horizontal B-scans of spectral-domain optical coherence tomography through the center of the fovea, demonstrating a small preserved ellipsoid zone island (red bracket) surrounded by retinal atrophy. The hyporeflective areas demonstrate the cystoid macular edema (asterisk).

hand, the Italian patient (ITA1: II1) was homozygous for a different homozygous haplotype of a size of approximately 13 Mb, indicating that the c.881G>A variant arose at least twice on 2 different haplotypes.

Expression Analysis of *CREB3* c.881G>A in Fibroblast Cells

The c.881G>A variant introduces a premature stop codon (p.Trp294*) in the terminal exon (exon 9) of *CREB3*, a gene that encodes a protein of 371 amino acids. Although most transcripts harboring premature stop codons are recognized and degraded by the nonsense-mediated mRNA decay surveillance pathway,[19] some premature stop codons, especially those occurring in terminal exons or in proximity to the end of the open reading frame, might escape degradation. To study the effect of nonsense-mediated mRNA decay on the *CREB3* transcript harboring the c.881G>A variant, we established fibroblast cell lines from 2 individuals with homozygous variants (MOL0072-4 and MOL0072-7) and a control individual and performed RT-PCR analysis with 9 sets of primers covering the 5′ untranslated region (5′ UTR) (part of exon 1), the open reading frame (exons 1-9), and the 3′ UTR (exon 9) of *CREB3* (eTable 1 in Supplement 1). The analysis showed that in fibroblasts, nonsense-mediated mRNA decay does not affect the expression levels of the transcripts harboring the c.881G>A variant (**Figure 3**A), and therefore, a truncated protein is likely to be produced. To examine this hypothesis, we performed Western blot analysis on protein extracts from fibroblast samples of the 2 patients and the control using a polyclonal

Figure 3. Expression Analysis for *CREB3* Using Reverse Transcription–Polymerase Chain Reaction (RT-PCR) and Western Blot

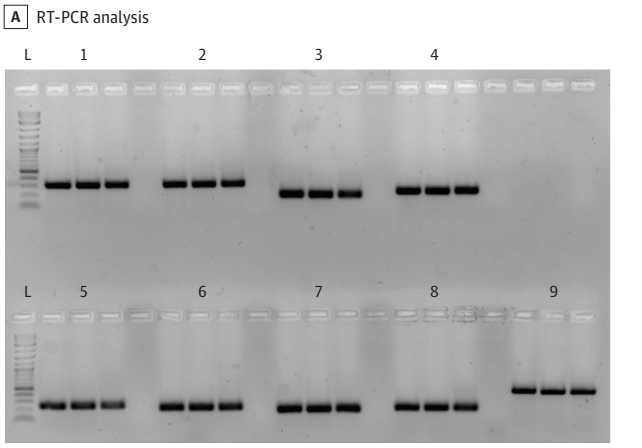

RT-PCR	Exons	Size, bp
1	5′UTR-EX2	316
2	EX1-EX3	320
3	EX2-EX4	203
4	EX3-EX5	242
5	EX4-EX7	250
6	EX5-EX8	224
7	EX7-EX9	205
8	EX8-EX9	219
9	EX8-3′UTR	465

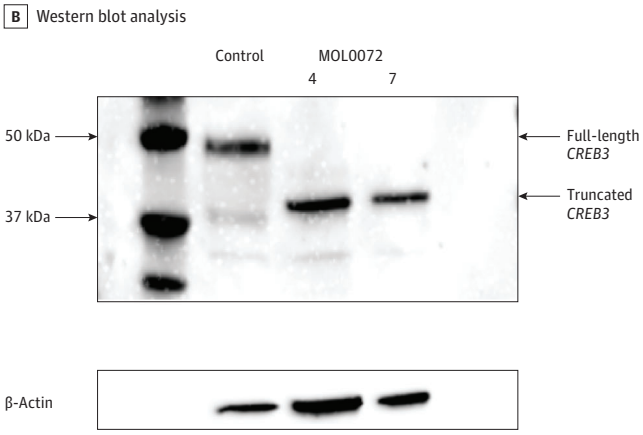

A, RT-PCR analysis of *CREB3* in fibroblast cells shows that variant *CREB3* evades nonsense-mediated mRNA decay surveillance pathway. RT-PCR amplification of 9 amplicons (RT-PCR 1 to 9) along the *CREB3* transcript is shown (primer sequences are shown in eTable 1 in Supplement 1). Each amplicon has been obtained independently from 3 samples (left to right): MOL0072-4 (homozygous variant), MOL0072-7 (homozygous variant), and control, followed by an RT-PCT negative control reaction. L indicates 100-bp ladder DNA marker. B, Western blot analysis of the CREB3 protein in control and homozygous variant dermal fibroblast cells. A single major band corresponding to the full-length protein is detected in the control sample, while a major band of lower mass is detected in the cells from the 2 homozygous patients corresponding to the truncated CREB3 protein. β-Actin was used as an internal control.

antibody against amino acids 1 through 230 of CREB3. We detected a band corresponding to a protein of approximately 50 KDa in the control sample, while a lower mass protein of approximately 40 KDa was evident in samples from individuals with c.881G>A homozygosity (Figure 3B). The bands corresponded to mass values that were higher than the expected molecular weight of the full-length protein (41.4 KDa) and of the truncated protein (33.1 KDa), probably due to N-linked glycosylation, as previously shown for CREB3[20] and CREB-H.[21]

Expression Analysis of *CREB3* in the Retina

To verify the expression of *CREB3* in the retina, we examined single-cell RNaseq data (based on a platform for analysis of scEiad).[22] The results (eFigure 2 in Supplement 1) show that *CREB3* was expressed in all retinal cell types, including rod and cone photoreceptors, with the highest expression level in amacrine, horizontal, and retinal ganglion cells.

We subsequently performed an immunohistological analysis of CREB3 in the wild-type mouse retina and observed clear staining of the antibody in all layers of the mouse retina (**Figure 4**) indicating *CREB3* expression in various retinal cell types with the most intense labeling at the outer plexiform layer, where synapses between photoreceptors and horizontal and bipolar cells are formed. The control slides were negative for CREB3-staining in all retinal layers.

Assessing the Genetic Prevalence of Null Variants in *CREB3*

Aiming to assess the distribution of *CREB3* null variants in various populations, we collected allele frequency data from gnomAD version 4.1.0 and included in our analysis only variants that were expected to be null. We identified 86 null variants: 41 frameshift, 23 canonical splice-site, and 22

Figure 4. Immunohistochemical Staining of CREB3 in the Wild-Type Mouse Retina

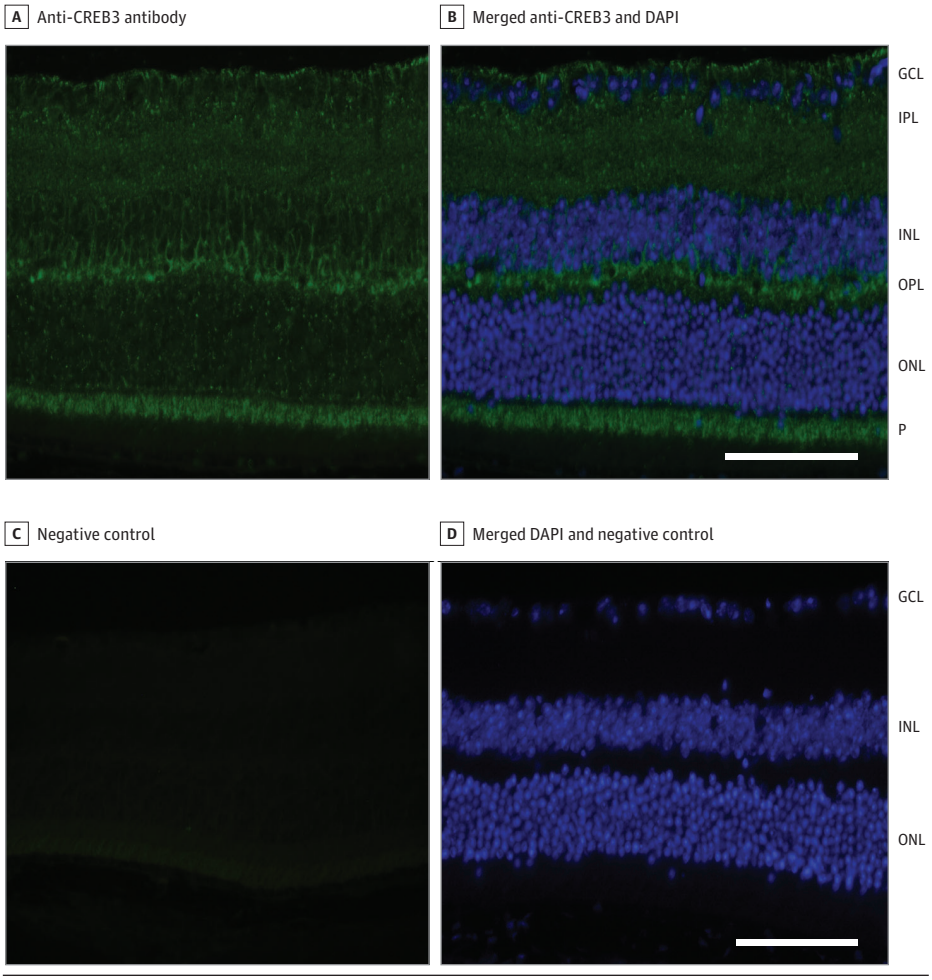

Both nuclear staining and membranal staining (green fluorescence) of the cell bodies are evident. A robust CREB3 staining was observed across all layers of the mouse retina, indicating the protein expression in multiple retinal cell types, with the strongest signal detected in the outer plexiform layer (OPL), where synaptic connections between photoreceptors, horizontal cells, and bipolar cells are established. Scale bar is 100 µm. GCL indicates ganglion cell layer; INL, inner nuclear layer; IPL, inner plexiform layer, OPL; ONL, outer nuclear layer; P, photoreceptors inner and outer segment.

nonsense variants. A total of 505 alleles were variated with a variant allele frequency of 0.0003 and a carrier frequency value of 1 for every 1596 individuals for all *CREB3* null variants combined. The expected genetic prevalence of biallelic *CREB3* cases is about 1 in 1 million individuals, with about 800 biallelic cases worldwide. Since the disease onset of *CREB3* biallelic cases is variable, it is expected that about half of individuals with biallelic variants might be affected.

The list of the 10 most common *CREB3* null variants is shown in eTable 2 in Supplement 1. The most common variant was c.281_282del, identified in 187 alleles, most of which (181) were of European origin. Its prevalence was higher than the remaining 9 *CREB3* null alleles combined, and therefore, we predict that once this gene is included in IRD WES and panel analyses, this variant is likely to be the most prevalent *CREB3* pathogenic variant worldwide. Non-null variants (mainly missense and in-frame) were not included in this analysis since there is currently no evidence for their pathogenicity. The c.881G>A variant reported here is not included on this list since it was detected on only 3 gnomAD alleles.

Discussion

Cyclic AMP response element binding protein-3 (CREB3), also known as LUMAN in humans or LZIP in mice, is an endoplasmic reticulum–membrane-bound transcription factor. On endoplasmic reticulum stress, CREB3 is shuttled to the Golgi apparatus where it is cleaved by S1P and S2P proteases to release the active N-terminus, which translocates to the nucleus and acts as a transcription factor.[23] CREB3 family members regulate the expression of a large variety of genes, and according to the tissue-specific expression profiles they play, among others, roles in acute phase response, lipid metabolism, development, survival, differentiation, organelle autoregulation, and protein secretion. They have been implicated in the endoplasmic reticulum and Golgi stress responses as regulators of the cell secretory capacity and cell-specific cargo.[24,25]

In this study, we report on an association of CREB3 with retinal dystrophies. We identified 13 patients from 4 different families, 3 of North-African Jewish descent, with homozygosity for a nonsense pathogenic variant, c.881G>A (p.Trp294*)

predicted to introduce a premature stop codon in the terminal exon, leading to a truncated protein product that is not degraded by nonsense-mediated mRNA decay, at least in fibroblast cells. It is well established that nonsense-mediated mRNA decay might not degrade premature stop codons situated in the terminal exon or those that are in close proximity to the termination codon.[26] It should be noted, however, that our analysis was done in fibroblast cells and therefore the results may not fully reflect the nonsense-mediated mRNA decay effect in the retina, as nonsense-mediated mRNA decay function was shown to vary among different tissues.[27]

Our expression and functional analyses of CREB3 show that it is crucial for photoreceptor function. However, due to the variable disease expression among patients with an identical *CREB3* genotype, we hypothesize that other internal or external factors may interfere with CREB3 function. These factors include (1) background variation in the genome that predisposes individuals to disease through disruption of physiological pathways or accumulation of polygenic effects or both combined; (2) the functional redundancy of genes and the location of the variant (for example, the p.Trp294* variant we identified introduces a stop codon at position 294, leading to a truncated protein in fibroblasts in which the 77 downstream amino acids are lost); (3) environmental factors, such as differences in the intensity and duration of exposure of patients to ultraviolet light, may cause variable retinal injury patterns given the reported involvement of CREB3 in protecting the retina from ultraviolet damage.[28]

CREB3 consists of 3 major functional domains[29]: the cytoplasmic domain that includes the transcription activation domain (aa 1-62), which mediates sequence-specific DNA binding and the leucine zipper domain (aa 162-223); the transmembrane domain that allows the association with the endoplasmic reticulum (aa 239-259), and the luminal domain (aa 259-379). In response to various signals, including endoplasmic reticulum stress, CREB3 is transported from the endoplasmic reticulum to the Golgi complex, where it is cleaved sequentially by the S1P and S2P proteases.[30] The cleaved CREB3 protein is then translocated into the nucleus and activates the transcription of target genes. The active form of CREB3 does not contain the transmembrane and luminal domains. The nonsense variant we identified results in a truncated domain (aa 1-294) that includes the cytoplasmic domain (which contains the regions that are active in the transcription of target genes) but lacks a major part of the luminal domain. The variant protein is therefore expected to have an abnormal function of sensing the activating signals, such as the endoplasmic reticulum stress, resulting in either a nonactivated CREB3 protein or a mutant isoform with malfunctioning transactivation properties. Additional experiments are needed to better characterize the effect of this truncated variant on CREB3 protein function and its relevance to the retina.

All 13 individuals we report here were homozygous for c.881G>A (p.Trp294*) and have a nonsyndromic IRD of variable severity, as reflected by the age at onset (ranging from 10 to 60 years) and the retinal phenotype (retinitis pigmentosa vs cone-rod dystrophy). Such clinical variability is not common in autosomal recessive IRDs and is usually explained by genotype-phenotype correlations.[31,32] However, clinical variability in patients carrying the same genotype has been reported in a few cases. Disease-causing variants in *CERKL* (eg, the founder disease-causing variant c.238 + 1G>A in Yemenite Jews) have been implicated in diverse phenotypic presentations, including typical retinitis pigmentosa, cone-rod dystrophy, or retinal degeneration accompanied by early macular degeneration in homozygous cases.[33] Another excellent example is *NR2E3*, which, when variated, can be associated with 4 retinal phenotypes (retinitis pigmentosa, enhanced S-cone syndrome, Goldmann-Favre syndrome, and clumped pigmentary retinal degeneration),[34,35] without a clear genotype-phenotype correlation. On the other hand, large clinical variability is evident in autosomal-dominant IRD genes, such as *PRPF31*, *PRPH2*, *RHO*, *BEST1*, and many others, and in the case of *PRPF31,* the mechanism for variability is partially understood and stems from variants in genes that regulate the expression of the wild-type *PRPF31* allele.[36-38] In general, both environmental (yet to be identified) and genetic variants in modifier genes are suspected to contribute to such clinical variability.

The *CREB3* c.881G>A variant was identified in 4 families, 3 of whom shared the same ethnicity, North-African Jews, leading us to hypothesize that c.881G>A is a founder pathogenic variant in this population. Only a limited number of founder variants have been reported to contribute to IRDs in this population, including variants in *RPE65*, *AIPL1*, and *GUCY2D*[39] (associated with Leber congenital amaurosis) and a variant in *FAM161A*[40] (associated with retinitis pigmentosa). Homozygosity mapping analysis on exome sequencing data revealed relatively large homozygous regions flanking *CREB3* with a shared haplotype, indicating that c.881G>A is indeed a founder pathogenic variant in the North African Jewish population.

Limitations

This study has several limitations, including the fact that it concentrates on a single homozygous nonsense variant, which limits insights into other potential pathogenic variants in *CREB3* or its pathway. Also, functional data were obtained from patient-derived fibroblasts rather than retinal tissue, which may not fully replicate retinal-specific gene regulation. In addition, while *CREB3* expression has been demonstrated in mouse retinal sections, no in vivo model shows the pathogenic effect of the *CREB3* variant on retinal degeneration.

Conclusion

To summarize, the findings in this study indicated that *CREB3* c.881G>A escapes nonsense-mediated mRNA decay on transcription, resulting in a shortened C-terminal that affects the function of the CREB3 protein. As a result, variable phenotypes of degenerated retina can be seen in patients with conditions ranging from retinitis pigmentosa (with or without macular involvement to cone-rod dystrophy). We observed this variable expressivity in 13 patients from 4 different families. The expression of *CREB3* in various human retinal cell types and the different layers of the mouse retina shows a clear correlation of genotype-phenotype.

ARTICLE INFORMATION

Accepted for Publication: April 29, 2025.

Published Online: July 17, 2025. doi:10.1001/jamaophthalmol.2025.2187

Author Affiliations: Department of Ophthalmology, Hadassah Medical Center, Faculty of Medicine, the Hebrew University of Jerusalem, Jerusalem, Israel. (Salameh, Abu Tair, Mousa, Obolensky, Banin, Sharon, Khateb); Neurobiology, Neurodegeneration and Repair Laboratory, National Eye Institute, Bethesda, Maryland (Swaroop); Human Genetics Department, Radboud University Medical Center, Nijmegen, the Netherlands (Roosing); Rappaport Faculty of Medicine, Technion-Israel Institute of Technology, Haifa, Israel (Mezer, Ben-Yosef); Department of Ophthalmology, Rambam Health Care Center, Haifa, Israel (Mezer); Department of Ophthalmology, Rabin Medical Center, Petah Tikva, Israel (Soudry); Department of Precision Medicine, University of Campania Luigi Vanvitelli, Naples, Italy (Karali, Banfi); Multidisciplinary Department of Medical, Surgical and Dental Sciences, Eye Clinic, University of Campania Luigi Vanvitelli, Naples, Italy (Karali, Simonelli); Telethon Institute of Genetics and Medicine, Pozzuoli, Italy (Banfi).

Author Contributions: Prof Sharon and Dr Khateb had full access to all of the data in the study and take responsibility for the integrity of the data and the accuracy of the data analysis. Mss Salameh and Abu Tair contributed equally. Prof Sharon and Dr Khateb contributed equally.
Concept and design: Salameh, Abu Tair, Simonelli, Sharon, Khateb.
Acquisition, analysis, or interpretation of data: Salameh, Abu Tair, Mousa, Obolensky, Swaroop, Roosing, Mezer, Soudry, Karali, Banfi, Banin, Ben-Yosef, Sharon, Khateb.
Drafting of the manuscript: Salameh, Abu Tair, Mousa, Karali, Khateb.
Critical review of the manuscript for important intellectual content: Salameh, Abu Tair, Mousa, Obolensky, Swaroop, Roosing, Mezer, Soudry, Simonelli, Banfi, Banin, Ben-Yosef, Sharon, Khateb.
Statistical analysis: Abu Tair, Mousa.
Obtained funding: Mousa, Obolensky, Swaroop, Roosing, Banfi, Banin, Sharon.
Administrative, technical, or material support: Salameh, Swaroop, Soudry, Banfi, Ben-Yosef, Khateb.
Supervision: Simonelli, Banin, Sharon, Khateb.

Conflict of Interest Disclosures: Mrs Salameh reported funding from the Neubauer Family Foundation and the Science Training Encouraging Peace Foundation. No other disclosures were reported.

Funding/Support: This research was supported by the Israel Science Foundation (grant 1778/20) within the Israel Precision Medicine Partnership program, the Foundation Fighting Blindness USA (grant BR-GE-0214-0639-TECH), the Yedidut Research Foundation, and the National Eye Institute (Z01EY000546). Mrs Salameh was funded by the Neubauer Family Foundation.

Role of the Funder/Sponsor: The funders had no role in the design and conduct of the study; collection, management, analysis, and interpretation of the data; preparation, review, or approval of the manuscript; and decision to submit the manuscript for publication.

Meeting Presentation: This work was presented at the 2nd International Electronic Conference on Genes (online); December 13, 2024; and the Association for Research in Vision and Ophthalmology annual meeting; May 5, 2025; Salt Lake City, Utah.

Data Sharing Statement: See Supplement 2.

Additional Contributions: We thank all patients and family members for their participation in this study. We also thank Sandeep Asodu, PhD, Department of Ophthalmology, Hadassah Medical Center, Faculty of Medicine, the Hebrew University of Jerusalem, Jerusalem, Israel, and Margherita Scarpato, PhD, Department of Precision Medicine, University of Campania Luigi Vanvitelli, Naples, Italy, for technical assistance and Francesco Testa, Multidisciplinary Department of Medical, Surgical and Dental Sciences, University of Campania Luigi Vanvitelli, Naples, Italy, for helpful discussion. No compensation or incentives were given for these contributions.

REFERENCES

1. Schneider N, Sundaresan Y, Gopalakrishnan P, et al. Inherited retinal diseases: linking genes, disease-causing variants, and relevant therapeutic modalities. *Prog Retin Eye Res*. 2022;89:101029. doi:10.1016/j.preteyeres.2021.101029

2. Hanany M, Rivolta C, Sharon D, Daiger SP. Worldwide carrier frequency and genetic prevalence of autosomal recessive inherited retinal diseases. *Proc Natl Acad Sci USA*. 2020;117(5):2710-2716. doi:10.1073/pnas.1913179117

3. Hanany M, Shalom S, Ben-Yosef T, Sharon D. Comparison of worldwide disease prevalence and genetic prevalence of inherited retinal diseases and variant interpretation considerations. *Cold Spring Harb Perspect Med*.2024;14(2):a041277. doi:10.1101/cshperspect.a041277

4. Han JH, Rodenburg K, Hayman T, et al. Loss-of-function variants in *UBAP1L* cause autosomal recessive retinal degeneration. *Genet Med*. 2024;26(6):101106. doi:10.1016/j.gim.2024.101106

5. Zeitz C, Navarro J, Azizzadeh Pormehr L, et al. Variants in *UBAP1L* lead to autosomal recessive rod-cone and cone-rod dystrophy. *Genet Med*. 2024;26(6):101081. doi:10.1016/j.gim.2024.101081

6. Bauwens M, Celik E, Zur D, et al. Mutations in *SAMD7* cause autosomal-recessive macular dystrophy with or without cone dysfunction. *Am J Hum Genet*. 2024;111(2):393-402. doi:10.1016/j.ajhg.2024.01.001

7. Bertrand RE, Wang J, Xiong KH, et al. Ceramide synthase *TLCD3B* is a novel gene associated with human recessive retinal dystrophy. *Genet Med*. 2021;23(3):488-497. doi:10.1038/s41436-020-01003-x

8. Ben-Yosef T. Inherited retinal diseases. *Int J Mol Sci*. 2022;23(21):13467. doi:10.3390/ijms232113467

9. Carss KJ, Arno G, Erwood M, et al; NIHR-BioResource Rare Diseases Consortium. Comprehensive rare variant analysis via whole-genome sequencing to determine the molecular pathology of inherited retinal disease. *Am J Hum Genet*. 2017;100(1):75-90. doi:10.1016/j.ajhg.2016.12.003

10. Hayman T, Millo T, Hendler K, et al. Whole exome sequencing of 491 individuals with inherited retinal diseases reveals a large spectrum of variants and identification of novel candidate genes. *J Med Genet*. 2024;61(3):224-231. doi:10.1136/jmg-2023-109482

11. Del Pozo-Valero M, Riveiro-Alvarez R, Martin-Merida I, et al. Impact of next generation sequencing in unraveling the genetics of 1036 spanish families with inherited macular dystrophies. *Invest Ophthalmol Vis Sci*. 2022;63(2):11. doi:10.1167/iovs.63.2.11

12. Karali M, Testa F, Di Iorio V, et al. Genetic epidemiology of inherited retinal diseases in a large patient cohort followed at a single center in Italy. *Sci Rep*. 2022;12(1):20815. doi:10.1038/s41598-022-24636-1

13. Weisschuh N, Sturm M, Baumann B, et al. Deep-intronic variants in *CNGB3* cause achromatopsia by pseudoexon activation. *Hum Mutat*. 2020;41(1):255-264. doi:10.1002/humu.23920

14. Hopiavuori BR, Anderson RE, Agbaga MP. *ELOVL4*: very long-chain fatty acids serve an eclectic role in mammalian health and function. *Prog Retin Eye Res*. 2019;69:137-158. doi:10.1016/j.preteyeres.2018.10.004

15. Lander ES, Botstein D. Homozygosity mapping: a way to map rare recessive traits using markers in linkage disequilibrium. *Genetics*. 1987;121(1):185-199.

16. Del Pozo-Valero M, Almoallem B, Dueñas Rey A, et al. Autozygome-guided exome-first study in a consanguineous cohort with early-onset retinal disease uncovers an isolated *RIMS2* phenotype and a retina-enriched *RIMS2* isoform. *Clin Genet*. 2024;106(2):127-139. doi:10.1111/cge.14517

17. Coppieters F, Ascari G, Dannhausen K, et al. Isolated and syndromic retinal dystrophy caused by biallelic mutations in *RCBTB1*, a gene implicated in ubiquitination. *Am J Hum Genet*. 2016;99(2):470-480. doi:10.1016/j.ajhg.2016.06.017

18. Madhangi M, Dutta D, Show S, et al. Exome sequencing and functional studies in zebrafish identify *WDR8* as the causative gene for isolated microspherophakia in Indian families. *Hum Mol Genet*. 2021;30(6):467-484. doi:10.1093/hmg/ddab061

19. Kurosaki T, Maquat LE. Nonsense-mediated mRNA decay in humans at a glance. *J Cell Sci*. 2016;129(3):461-467. doi:10.1242/jcs.181008

20. Raggo C, Rapin N, Stirling J, et al. Luman, the cellular counterpart of herpes simplex virus VP16, is processed by regulated intramembrane proteolysis. *Mol Cell Biol*. 2002;22(16):5639-5649. doi:10.1128/MCB.22.16.5639-5649.2002

21. Chan CP, Mak TY, Chin KT, Ng IOL, Jin DY. N-linked glycosylation is required for optimal proteolytic activation of membrane-bound transcription factor CREB-H. *J Cell Sci*. 2010;123(Pt 9):1438-1448. doi:10.1242/jcs.067819

22. Swamy VS, Fufa TD, Hufnagel RB, McGaughey DM. Building the mega single-cell transcriptome ocular meta-atlas. *Gigascience*. 2021;10(10):giab061. doi:10.1093/gigascience/giab061

23. Lu R, Misra V. Potential role for luman, the cellular homologue of herpes simplex virus VP16 (α gene trans-inducing factor) in herpesvirus latency.

J Virol. 2000;74(2):934-943. doi:10.1128/jvi.74.2.934-943.2000

24. Sampieri L, Di Giusto P, Alvarez C. CREB3 transcription factors: ER-golgi stress transducers as hubs for cellular homeostasis. *Front Cell Dev Biol*. 2019;7:123. doi:10.3389/fcell.2019.00123

25. Smith BS, Diaguarachchige De Silva KH, Hashemi A, et al. Transcription factor CREB3 is a potent regulator of high-fat diet-induced obesity and energy metabolism. *Int J Obes (Lond)*. 2022;46(8):1446-1455. doi:10.1038/s41366-022-01128-w

26. Mort M, Ivanov D, Cooper DN, Chuzhanova NA. A meta-analysis of nonsense mutations causing human genetic disease. *Hum Mutat*. 2008;29(8):1037-1047. doi:10.1002/humu.20763

27. Zetoune AB, Fontanière S, Magnin D, et al. Comparison of nonsense-mediated mRNA decay efficiency in various murine tissues. *BMC Genet*. 2008;9:83. doi:10.1186/1471-2156-9-83

28. An MJ, Kim CH, Nam GY, et al. Transcriptome analysis for UVB-induced phototoxicity in mouse retina. *Environ Toxicol*. 2018;33(1):52-62. doi:10.1002/tox.22494

29. Liang G, Audas TE, Li Y, et al. Luman/CREB3 induces transcription of the endoplasmic reticulum (ER) stress response protein Herp through an ER stress response element. *Mol Cell Biol*. 2006;26(21):7999-8010. doi:10.1128/MCB.01046-06

30. McCurdy EP, Chung KM, Benitez-Agosto CR, Hengst U. Promotion of axon growth by the secreted end of a transcription factor. *Cell Rep*. 2019;29(2):363-377.e5. doi:10.1016/j.celrep.2019.08.101

31. Ash JD, Pierce E, Anderson RE, Bowes Rickman C, Hollyfield JG, Grimm C, eds. *Retinal Degenerative Diseases XIX*. Springer Cham; 2019.

32. Hufnagel RB, Liang W, Duncan JL, et al; Foundation Fighting Blindness Consortium Investigator Group. Tissue-specific genotype-phenotype correlations among USH2A-related disorders in the RUSH2A study. *Hum Mutat*. 2022;43(5):613-624. doi:10.1002/humu.24365

33. Auslender N, Sharon D, Abbasi AH, Garzozi HJ, Banin E, Ben-Yosef T. A common founder mutation of *CERKL* underlies autosomal recessive retinal degeneration with early macular involvement among Yemenite Jews. *Invest Ophthalmol Vis Sci*. 2007;48(12):5431-5438. doi:10.1167/iovs.07-0736

34. Sharon D, Sandberg MA, Caruso RC, Berson EL, Dryja TP. Shared mutations in NR2E3 in enhanced S-cone syndrome, Goldmann-Favre syndrome, and many cases of clumped pigmentary retinal degeneration. *Arch Ophthalmol*. 2003;121(9):1316-1323. doi:10.1001/archopht.121.9.1316

35. Schorderet DF, Escher P. *NR2E3* mutations in enhanced S-cone sensitivity syndrome (ESCS), Goldmann-Favre syndrome (GFS), clumped pigmentary retinal degeneration (CPRD), and retinitis pigmentosa (RP). *Hum Mutat*. 2009;30(11):1475-1485. doi:10.1002/humu.21096

36. Venturini G, Rose AM, Shah AZ, Bhattacharya SS, Rivolta C. *CNOT3* is a modifier of *PRPF31* mutations in retinitis pigmentosa with incomplete penetrance. *PLoS Genet*. 2012;8(11):e1003040. doi:10.1371/journal.pgen.1003040

37. Rio Frio T, Wade NM, Ransijn A, Berson EL, Beckmann JS, Rivolta C. Premature termination codons in *PRPF31* cause retinitis pigmentosa via haploinsufficiency due to nonsense-mediated mRNA decay. *J Clin Invest*. 2008;118(4):1519-1531. doi:10.1172/JCI34211

38. Rivolta C, McGee TL, Rio Frio T, Jensen RV, Berson EL, Dryja TP. Variation in retinitis pigmentosa-11 (*PRPF31* or *RP11*) gene expression between symptomatic and asymptomatic patients with dominant *RP11* mutations. *Hum Mutat*. 2006;27(7):644-653. doi:10.1002/humu.20325

39. Banin E, Bandah-Rozenfeld D, Obolensky A, et al. Molecular anthropology meets genetic medicine to treat blindness in the North African Jewish population: human gene therapy initiated in Israel. *Hum Gene Ther*. 2010;21(12):1749-1757. doi:10.1089/hum.2010.047

40. Bandah-Rozenfeld D, Mizrahi-Meissonnier L, Farhy C, et al. Homozygosity mapping reveals null mutations in *FAM161A* as a cause of autosomal-recessive retinitis pigmentosa. *Am J Hum Genet*. 2010;87(3):382-391. doi:10.1016/j.ajhg.2010.07.022